Multimodal MRI reveals brainstem connections that sustain wakefulness in human consciousness

Brian L. Edlow[1,2,*], Mark Olchanyi[1,3], Holly J. Freeman[1,2], Jian Li[1,2], Chiara Maffei[1,2], Samuel B. Snider[4], Lilla Zöllei[2], J. Eugenio Iglesias[2], Jean Augustinack[2], Yelena G. Bodien[1,5], Robin L. Haynes[6], Douglas N. Greve[2], Bram R. Diamond[1,2], Allison Stevens[2], Joseph T. Giacino[5], Christophe Destrieux[7,8], Andre van der Kouwe[2], Emery N. Brown[9,10], Rebecca D. Folkerth[11], Bruce Fischl[2], Hannah C. Kinney[6]

[1] Center for Neurotechnology and Neurorecovery, Department of Neurology, Massachusetts General Hospital and Harvard Medical School, Boston, MA, USA.
[2] Athinoula A. Martinos Center for Biomedical Imaging, Department of Radiology, Massachusetts General Hospital and Harvard Medical School, Charlestown, MA, USA.
[3] Institute for Medical Engineering and Science, Massachusetts Institute of Technology, Cambridge, MA, USA.
[4] Department of Neurology, Brigham and Women's Hospital and Harvard Medical School, Boston, MA, USA.
[5] Department of Physical Medicine and Rehabilitation, Spaulding Rehabilitation Hospital and Harvard Medical School, Charlestown, MA, USA.
[6] Department of Pathology, Boston Children's Hospital and Harvard Medical School, Boston, MA, USA.
[7] UMR 1253, iBrain, Université de Tours, Inserm, Tours, France.
[8] CHRU de Tours, Tours, France.
[9] Department of Anesthesia, Critical Care, and Pain Medicine, Massachusetts General Hospital and Harvard Medical School, Boston, MA, USA.
[10] Department of Brain and Cognitive Sciences, Massachusetts Institute of Technology, Cambridge, MA, USA.
[11] Office of the Chief Medical Examiner, New York, NY, USA.
* Corresponding author. Email: bedlow@mgh.harvard.edu

Authors' accepted version
For research purpose only
Copyright (c) the publisher
Full article and citation at
https://doi.org/10.1126/scitranslmed.adj4303

ABSTRACT

Consciousness is composed of arousal (i.e., wakefulness) and awareness. Substantial progress has been made in mapping the cortical networks that underlie awareness in the human brain, but knowledge about the subcortical networks that sustain arousal in humans is incomplete. Here, we aimed to map the connectivity of a proposed subcortical arousal network that sustains wakefulness in the human brain, analogous to the cortical default mode network (DMN) that has been shown to contribute to awareness. We integrated data from ex vivo diffusion magnetic resonance imaging (MRI) of three human brains, obtained at autopsy from neurologically normal individuals, with immunohistochemical staining of subcortical brain sections. We identified nodes of the proposed default ascending arousal network (dAAN) in the brainstem, hypothalamus, thalamus, and basal forebrain. Deterministic and probabilistic tractography analyses of the ex vivo diffusion MRI data revealed projection, association, and commissural pathways linking dAAN nodes with one another and with DMN nodes. Complementary analyses of in vivo 7-tesla resting-state functional MRI data from the Human Connectome Project identified the dopaminergic ventral tegmental area in the midbrain as a widely connected hub node at the nexus of the subcortical arousal and cortical awareness networks. Our network-based autopsy methods and connectivity data provide a putative neuroanatomic architecture for the integration of arousal and awareness in human consciousness.

Authors' accepted version
For research purposes only
Copyright (C) the publisher
Full article and citation at
https://doi.org/10.1126/sciadv.adq4305

INTRODUCTION

To treat disorders of human consciousness, such as coma, vegetative state, and minimally conscious state, it is essential to understand the neuroanatomic determinants and interconnectivity of arousal and awareness, two foundational components of consciousness (*1*). Arousal refers to physiologic activation of the brain to a state of wakefulness (*2*), whereas awareness refers to the content of consciousness (*3*, *4*), which arises from the integration of unimodal, heteromodal, and paralimbic inputs (*5*). These two components of consciousness, arousal and awareness, can be dissociated, as observed in patients in the vegetative state, who demonstrate alternating cycles of wakefulness but absent awareness (*6*). Such clinical observations, bolstered by experimental data in animals (*7*–*9*), support the concept that the anatomic pathways of awareness and arousal are anatomically dissociated from one another in the brain.

Current concepts of consciousness propose that the cerebral cortex is the primary anatomic site of the neural correlates of awareness (*4*, *10*), whereas ascending subcortical pathways from the brainstem, hypothalamus, thalamus, and basal forebrain are the neural correlates of arousal (*11*, *12*). Over the past two decades, there has been substantial progress in mapping the cortical brain networks that mediate human awareness (*4*, *13*, *14*). In contrast, connectivity maps of subcortical networks that mediate human arousal are far less complete. This gap in knowledge is partly attributable to inadequate spatial resolution of standard neuroimaging techniques, which cannot discriminate individual arousal nuclei within the brainstem or delineate complex trajectories of axonal connections that link the brainstem to the diencephalon, basal forebrain, and cerebral cortex. In the absence of adequate imaging techniques for detecting brainstem arousal nuclei and their

axonal connections, subcortical arousal network mapping has stalled, whereas cortical awareness network mapping has accelerated. The few human studies of brainstem arousal nuclei generally support Moruzzi and Magoun's (*15*) seminal observations in cats regarding the key role of the brainstem reticular formation in activating the cerebral cortex. Positron emission tomography (PET) studies have identified an increase in metabolic activity within the brainstem reticular formation when humans wake from sleep (*16*). Similarly, PET studies have revealed altered metabolism within the reticular formation in patients with disorders of consciousness caused by severe brain injuries (*17*).

Beyond the reticular formation, animal and human studies have revealed that extrareticular nuclei in the brainstem (*7*, *18–21*), as well as nuclei in the hypothalamus (*8*, *22*, *23*), thalamus (*24*, *25*), and basal forebrain (*7*, *26*, *27*), also contribute to arousal (*7*, *28*, *29*). Collectively, these observations suggest that the human ascending arousal network (AAN) is a synchronized, multi-transmitter brain network composed of reticular and extrareticular nuclei that generate activated states of alertness in response to multiple external stimuli, including noxious, tactile, vestibular, olfactory, auditory, thermal, and homeostatic stimuli (e.g., hypoxia and hypercarbia). We investigated the anatomic substrate of the AAN that modulates the default state of resting wakefulness, which we refer to as the default AAN (dAAN).

Default modes of brain activity involve neuronal ensembles that create distinct oscillatory modes of firing patterns during different brain states (*30*). In the awake state, the brain toggles between a default mode of wakefulness (i.e., resting wakefulness) and a non-default mode of wakefulness (i.e., active attention or task performance) (*10*, *31*). In this conceptual framework, a default network is one whose nodes demonstrate temporally correlated activity during a default mode of brain activity (*32*). dAAN nodes may also modulate internally and externally directed cognitive processes, just as default mode network (DMN) nodes participate in a wide range of cognitive processes beyond self-awareness (*10*), but our focus is on maintenance of the resting wakeful state, which requires input from the dAAN.

This view of a default state of arousal is consistent with that expressed by Steriade and Buzsaki (*33*), who wrote that "operationally, arousal may be defined as a standby mode of the neurons for efficient processing and transformation of afferent information." In the "standby mode" of resting wakefulness, the human brain is not performing an externally or internally directed (i.e., introspective) task. Instead, the resting state provides conditions for forms of cognition that do not rely on external signals as input (*34*, *35*). Behaviorally, the eyes may be open or closed. Electrophysiologically, subcortical arousal neurons fire tonically (*36*), and the cerebral cortex generates desynchronized, high-frequency, low-voltage waves detected by electroencephalography (*2*). The dAAN thus sustains cortical activation to enable awareness, without requiring sensory input or externally directed cognition.

To advance knowledge about the connectivity of this subcortical default brain network critical to human consciousness, we performed a multimodal brain imaging study, integrating data from ex vivo diffusion magnetic resonance imaging (MRI) tractography and in vivo 7-tesla (7-T)

Authors' accepted version
For research purposes only
Copyright (c) the publisher
Full article and citation at
https://doi.org/10.1126/scitranslmed.abi4303

functional MRI (fMRI). We used histology and immunohistochemistry guidance to identify the anatomic location of dAAN nodes on ex vivo MRI scans of three human brain specimens and then mapped the structural connections of the dAAN using diffusion MRI tractography at submillimeter spatial resolution. We then performed resting-state fMRI analyses of 7-T imaging data from the Human Connectome Project (*37*) to investigate the functional correlates of these structural connections. The complementary structural-functional connectivity analyses aimed to identify the neuroanatomic basis for the integration of arousal and awareness in the resting, conscious human brain.

RESULTS

Candidate dAAN nodes and structural connectivity

On the basis of evidence from previously published electrophysiological, gene expression, lesion, and stimulation studies, we identified 18 candidate dAAN nodes: 10 in the brainstem, 3 in the thalamus and hypothalamus, and 2 in the basal forebrain (Table S1). All 18 candidate nodes were located at the level of, or rostral to, the mid-pons. For the 13 nodes with available electrophysiological data—except for periaqueductal gray (PAG), pontis oralis (PnO), parabrachial complex (PBC), paraventricular nucleus (PaV), and supramammillary nucleus (SUM)—the electrophysiological evidence indicated active tonic firing of neurons during wakefulness and state-dependent changes in neuronal firing during wakefulness compared with slowwave sleep (Table S1).

Once the 18 candidate dAAN nodes were identified, we investigated their structural connectivity using ex vivo diffusion MRI tractography of three human brain specimens obtained at autopsy from neurologically normal individuals. The three brains were from women who died at ages 53, 60, and 61 years (Figs. S1 to S3). Demographic and clinical data, including the cause of death, are provided in Table S2. At autopsy, all three brain specimens had a normal fresh brain weight. Time from death until fixation in 10% formaldehyde ranged from 24 to 72 hours, a time window that is associated with preservation of directional water diffusion within formaldehydefixed brain tissue (*38*).

For specimen 1, candidate dAAN nodes were traced on the diffusion-weighted MRI images using guidance from serial histologic brain sections (stained with hematoxylin and eosin and counterstained with Luxol fast blue) and selected immunohistochemically stained brain sections (stained for tyrosine hydroxylase, a marker of dopaminergic neurons, and tryptophan hydroxylase, a marker of serotonergic neurons). Each set of diffusion images [diffusionweighted images, apparent diffusion coefficient map, fractional anisotropy (FA) map, color FA map, and non-diffusion weighted images (b = 0)] was compared to the corresponding stained brain sections to ensure that radiologic dAAN nodes shared the same location and morphology as the dAAN nuclei identified by histology and immunohistochemistry (Fig. 1 and Figs. S4 and S5). For brain specimens 2 and 3, the brainstem dAAN nuclei were traced manually on each diffusion MRI dataset with reference to selected histologic and immunohistochemically stained brain sections

Authors' accepted version
For research purposes only
Copyright (c) the publisher
Full article and citation at
https://doi.org/10.1126/scitranslmed.adj1308

and canonical atlases (*39*, *40*). The neuroanatomic boundaries of all candidate dAAN nodes are detailed in Tables S3 to S7, and three-dimensional (3D) visualizations of all candidate dAAN nodes in the three postmortem brain specimens are provided in Figs. S6 to S8. The candidate dAAN nodes are also shown in Montreal Neurological Institute (MNI) space, as version 2.0 of the Harvard ascending arousal network atlas (*11*), in movie S1. Our anatomical approach is presented in Supplementary Materials and Methods.

Brain specimen 1 was scanned at 600-μm resolution as a dissected specimen, consisting of the rostral pons, midbrain, hypothalamus, thalamus, basal forebrain, and part of the basal ganglia (*11*). Brain specimens 2 and 3 were scanned at 750-μm resolution as whole brains. Diffusion MRI data from all three specimens were processed for deterministic fiber tracking for qualitative assessment of tract trajectories, and diffusion data from specimens 2 and 3 were processed for probabilistic fiber tracking for quantitative assessment of connectivity. Probabilistic data for brain specimen 1 were not analyzed because differences in scanning parameters and specimen composition (i.e., dissected versus whole brain) precluded quantitative comparison.

Criteria for structural connectivity and anatomic classification of dAAN pathways

Structural connectivity was defined using a two-step process that incorporated the quantitative probabilistic data and qualitative deterministic data. First, we performed a quantitative assessment for the presence of a connection linking each node-node pair using the probabilistic data from brain specimens 2 and 3. A quantitative connection required a connectivity probability (CP) whose 95% confidence interval (CI) exceeded the 95% CI of CP values for two control regions, the basis pontis and red nucleus, that were unlikely to have connectivity with dAAN nodes based on prior animal labeling studies (*41*). If this a priori criterion was met in the probabilistic analysis, then we qualitatively assessed the deterministic tractography data for all three brain specimens for visual confirmation of tracts connecting each pair of candidate nodes. Node-node pairs that met both the probabilistic and deterministic criteria were considered to have inferential evidence for a structural connection, whereas node-node pairs that met one, but not both, criteria were considered to have uncertain connectivity.

We then classified the structural connectivity between all candidate node-node pairs on the basis of the anatomic trajectories and nomenclature of subcortical bundles previously defined in humans and animals (*11*, *42*): DTT_L, dorsal tegmental tract lateral division; DTT_M, dorsal tegmental tract medial division; LFB, lateral forebrain bundle; MFB, medial forebrain bundle; VTT_C, ventral tegmental tract caudal division; and VTT_R, ventral tegmental tract rostral division (Fig. 1). Next, we classified all dAAN pathways as association, commissural, or projection, providing a neuroanatomic taxonomy for the subcortical dAAN akin to that of cortical networks whose connections are classified in these terms (*43*). Using the brainstem as the frame of reference for classifying dAAN pathways, we defined association fibers as those that connect brainstem nuclei to ipsilateral brainstem nuclei and commissural fibers as those that crossed the midline to connect with contralateral brainstem nuclei. Projection fibers projected from brainstem nuclei to rostral diencephalic nuclei, basal forebrain nuclei, or DMN cortical regions that contribute to

Authors' accepted version
For research purposes only
Copyright (c) the publisher
Full article and citation at
https://doi.org/10.1126/sciadv.adj1308

consciousness (Fig. S9). Multiple cortical networks beyond the DMN, such as the salience and executive control networks (Fig. S10), contribute to conscious awareness (*44*). Our focus on dAAN-DMN connectivity was intended as a starting point for mapping the connections that integrate arousal and awareness in the human brain.

Projection pathways of the dAAN

Deterministic diffusion MRI tractography analysis of the three brain specimens revealed that tracts emanating from all dAAN candidate brainstem nuclei formed well-defined projection pathways that coursed through the rostral brainstem, diencephalon, and forebrain. Each pathway contained intermingled tracts from reticular nuclei (i.e., pontine and midbrain reticular formations) and

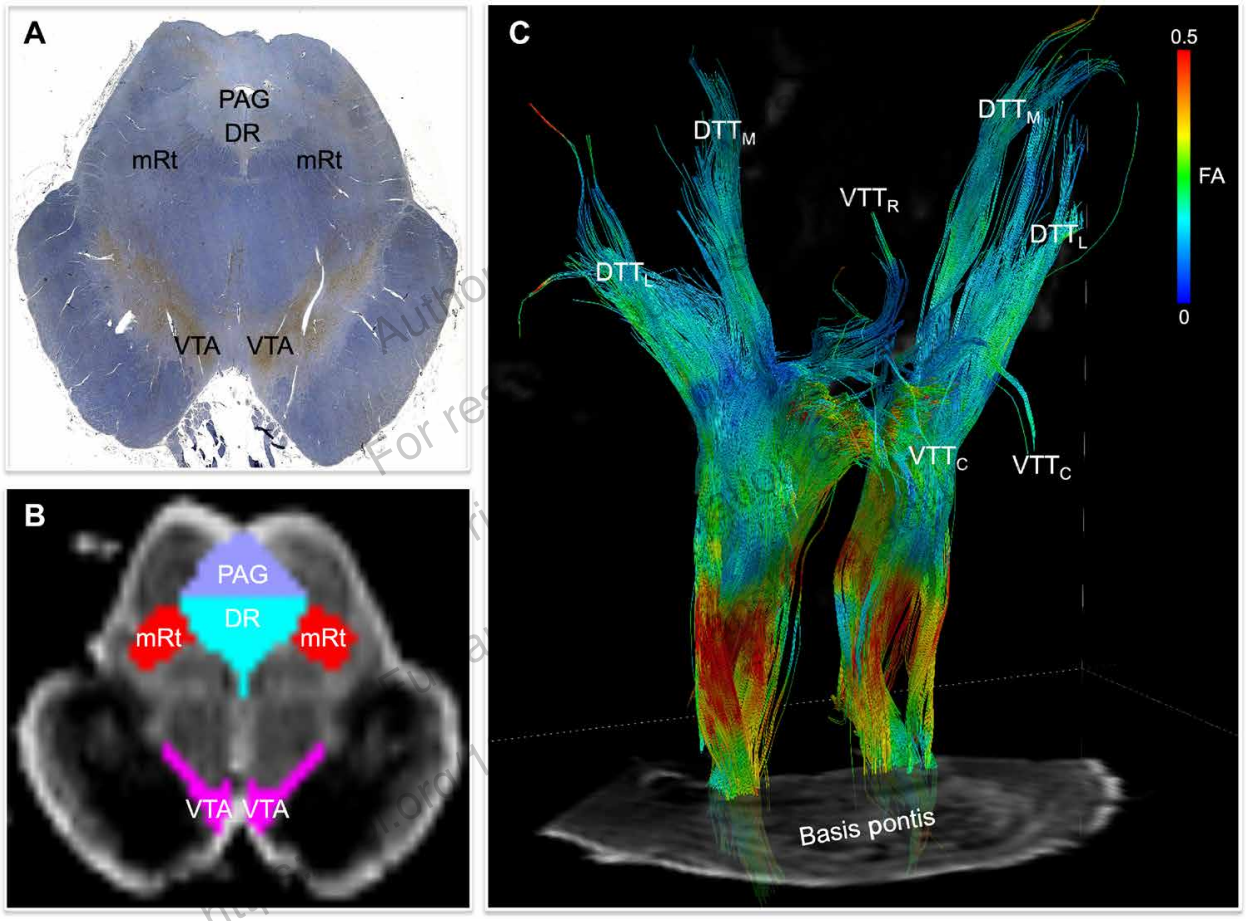

Fig. 1. Histological guidance for node localization and tract construction. (A) A transverse section through the caudal midbrain of brain specimen 1 is shown, stained with tyrosine hydroxylase and counterstained with hematoxylin. The tyrosine hydroxylase stain identifies dopaminergic neurons of the VTA. (B) The corresponding non–diffusion-weighted (b = 0) axial image from the same specimen is shown. VTA neurons are manually traced in pink on the basis of the tyrosine hydroxylase staining results, and additional arousal nuclei are traced on the basis of the hematoxylin and eosin/Luxol fast blue stain results. (C) Deterministic tractography results from a seed region in the mRt (15) are shown from a right ventrolateral perspective in brain specimen 1. Tracts are color-coded by the FA along each segment (color bar). Tracts are superimposed upon a b = 0 axial image at the level of the mid-pons. Fiber tracts emanating from mRt travel in the ponto-mesencephalic tegmentum and connect with the thalamus, hypothalamus, and basal forebrain via the following bundles: DTT_L, DTT_M, VTT_C, and VTT_R.

extrareticular nuclei (e.g., monoaminergic, cholinergic, and glutamatergic nuclei), although the distributions of reticular and extrareticular tracts within each pathway differed (Fig. 2).

All candidate brainstem nodes connected with at least one candidate hypothalamic, thalamic, or basal forebrain node based on CI testing (Table 1). Quantitative connectivity data are provided in Tables S8 to S11 for all projection pathways. The projection pathways that connected candidate brainstem dAAN nodes with thalamic, hypothalamic, and basal forebrain dAAN nodes are shown in Fig. 2. The projection pathways connecting candidate brainstem dAAN nodes with cortical DMN nodes are shown in Fig. 3. A projection fiber connectogram with averaged CP values for brain specimens 2 and 3 is shown in Fig. 4.

The qualitative trajectories of projection pathways connecting these nodes, as assessed by deterministic tractography, were consistent in all three brain specimens. All midbrain candidate nodes connected with the intralaminar nuclei of the thalamus (IL) via DTT_M and with PaV via VTT_R (Figs. 2 and 4 and Table 1). All midbrain nodes except the ventral tegmental area (VTA),

Authors' accepted version
For research purpose only
Copyright (c) the publisher
Full article and citation at
https://doi.org/10.1126/sciadv.adi4302

Table 1. Projection pathways connecting brainstem dAAN nodes with thalamic, hypothalamic, and basal forebrain dAAN nodes, as well as cortical DMN nodes. For connections that met both the probabilistic and deterministic criteria for a structural connection, we assessed the deterministic fiber tracts linking each pair of nodes for their anatomic trajectories and classified them using previously defined nomenclature (11, 42): DTT_L, DTT_M, LFB, MFB, VTT_C, VTT_R. If two nodes did not meet the criteria for a connection using the probabilistic or determinist criteria, then the label "---" is given to indicate the absence of a connection. If two nodes met criteria for a connection in the probabilistic or deterministic analysis but not both analyses, then the label "UC" (uncertain) is given.

Brain stem Node	Thalamus			Hypothalamus			Basal Forebrain		Default Mode Network				
	IL	Ret*	PaV	TMN	LHA	SUM	BNM/ SI	DBB	PMC	MPFC	IPL	LT	MT
mRt	DTT_M	DTT_L DTT_M	VTT_R	VTT_C	VTT_C	VTT_C	VTT_C	VTT_C	LFB	MFB	LFB	UC	LFB
VTA	DTT_M	UC	VTT_R	VTT_C	VTT_C	VTT_C	VTT_C	UC	LFB	MFB	LFB	LFB	LFB
PAG	DTT_M	DTT_L DTT_M	VTT_R	---	VTT_C	VTT_C	VTT_C	VTT_C	LFB	UC	LFB	LFB	LFB
PTg	DTT_M	DTT_L DTT_M	VTT_R	VTT_C	VTT_C	VTT_C	VTT_C	VTT_C	LFB	MFB	UC	LFB	LFB
DR	DTT_M	DTT_L	VTT_R	VTT_C	VTT_C	VTT_C	VTT_C	VTT_C	LFB	UC	UC	UC	LFB
PnO	DTT_M	DTT_L DTT_M	---	---	VTT_C	---	VTT_C	---	LFB	MFB	UC	UC	---
PBC	DTT_M	DTT_L DTT_M	UC	VTT_C	VTT_C	---	VTT_C	UC	LFB	MFB	LFB	UC	UC
MnR	---	---	---	---	VTT_C	---	VTT_C	---	LFB	MFB	LFB	UC	---
LC	UC	UC	UC	VTT_C	VTT_C	VTT_C	VTT_C	UC	LFB	UC	UC	UC	UC
LDTg	UC	UC	---	VTT_C	VTT_C	VTT_C	UC	VTT_C	UC	UC	UC	UC	UC

* The DTT_L pathway connects directly with the Ret, whereas the DTTM pathway connects with Ret after passing through the IL.

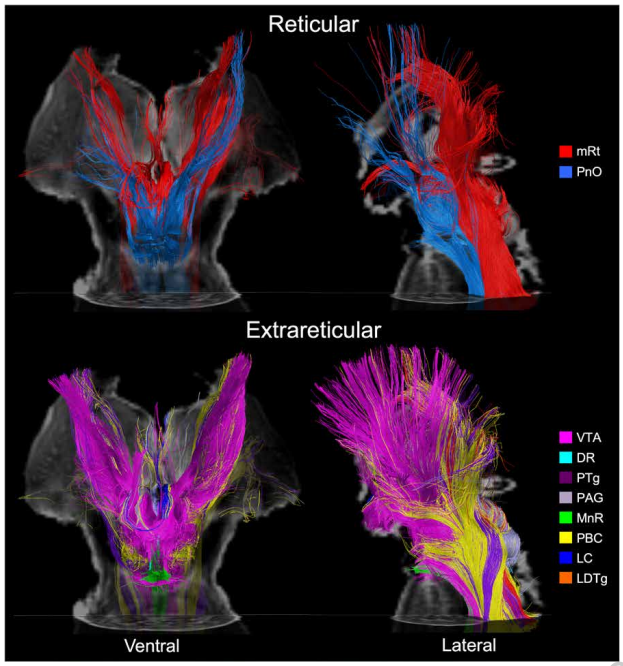

Fig. 2. Reticular and extrareticular tracts of the dAAN. Deterministic fiber tracts emanating from the reticular and extrareticular arousal nuclei are shown in the top and bottom panels, respectively. All tracts are from brain specimen 1 and superimposed on an axial non–diffusion-weighted (b=0) image at the level of the mid-pons. In addition, the tracts in the ventral perspective (left column) are superimposed on a coronal b=0 image at the level of the mid-thalamus, and the tracts in the left lateral perspective (right column) are superimposed on a sagittal b=0 image located at the midline. All tracts are color-coded according to their nucleus of origin (color key, right).

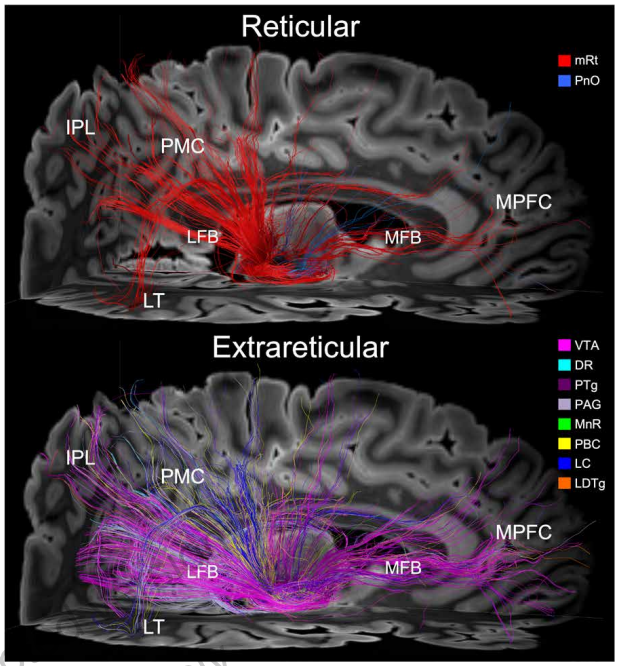

Fig. 3. Connections linking brainstem dAAN nodes with cortical DMN nodes. Deterministic fiber tracts emanating from the reticular and extrareticular arousal nuclei are shown in the top and bottom panels, respectively. All tracts are from brain specimen 2 and are shown from a right lateral perspective, superimposed on an axial non–diffusion-weighted (b=0) image at the level of the rostral midbrain, a sagittal b=0 image to the right of the midline, and a coronal b=0 image at the IPL. Tract colors are the same as in Fig. 2. Both the reticular and extrareticular brainstem arousal nuclei connect extensively with cortical nodes of the DMN, including the MPFC, PMC (i.e., posterior cingulate cortex and precuneus), IPL, and LT. The primary pathway that connects the brainstem arousal nuclei to MPFC is the MFB. The primary pathway that connects the brainstem arousal nuclei to the PMC, IPL, and LT is the LFB.

Author's accepted manuscript. For research purposes only. Copyright (c) the author/publisher. Full article and supplement at https://doi.org/10.1126/sciadv.adj4905

which showed uncertain connectivity, connected with the reticular nucleus of the thalamus (Ret) via DTT_L. Connectivity between pontine candidate nodes and the thalamic candidate nodes was more limited, with only PnO and PBC connecting with IL and Ret, and with the median raphe (MnR), locus coeruleus (LC), and laterodorsal tegmental nucleus (LDTg) showing either absent or uncertain connectivity with thalamic nodes (Figs. 2 and 4 and Table 1).

Structural connectivity with all three candidate hypothalamic nodes—tuberomammillary nucleus (TMN), lateral hypothalamic area (LHA), and SUM—via VTT_C was observed for midbrain reticular formation (mRt), VTA, pedunculotegmental nucleus (PTg), dorsal raphe (DR), LC, and LDTg, whereas other brainstem nuclei connected with one (PnO and MnR) or two (PAG and PBC) candidate hypothalamic nodes (Figs. 2 and 4 and Table 1). All midbrain and pontine candidate nodes connected with the LHA node of the hypothalamus via VTT_C (Fig. 4 and Table 1). Structural

connectivity with the basal nucleus of Meynert/substantia innominata (BNM/ SI) node of the basal forebrain was observed for all midbrain and pontine candidate nodes except LDTg via VTT_C (Fig. 4 and Table 1). All brainstem nodes except VTA, PnO, PBC, MnR, and LC connected with the diagonal band of Broca (DBB) node of the basal forebrain via VTT_C (Fig. 4 and Table 1).

All cortical DMN nodes (Figs. S11 and S12) showed structural connectivity with at least 3 of the 10 candidate brainstem dAAN nodes. The posteromedial complex (PMC; i.e., posterior cingulate cortex and precuneus) was the DMN node with the most extensive connections to brainstem dAAN nodes (all except LDTg) via the LFB. The medial prefrontal cortex (MPFC) node of the DMN was connected with all brainstem dAAN nodes except PAG, DR, LC, and LDTg via the MFB. The inferior parietal lobule (IPL) node of the DMN connected with mRt, VTA, PAG, PBC, and MnR via LFB. The medial temporal node of the DMN was connected with all midbrain nodes via a temporal branch of the LFB, and the lateral temporal node of the DMN was connected with all midbrain nodes except mRt. There were no connections between the lateral temporal and medial temporal nodes and the pontine candidate dAAN nodes. We observed a large contribution of extrareticular connections, dominated by VTA tracts, to the MPFC via the MFB (Fig. 3). Brainstem connections with IPL and PMC traveled in a parietal branch of the LFB, with similar connectivity contributions from VTA, PAG, and mRt (Fig. 3).

In a post hoc analysis, probabilistic dAAN-DMN connectivity measurements were similar to measurements between dAAN nodes and the six remaining cortical networks derived from the

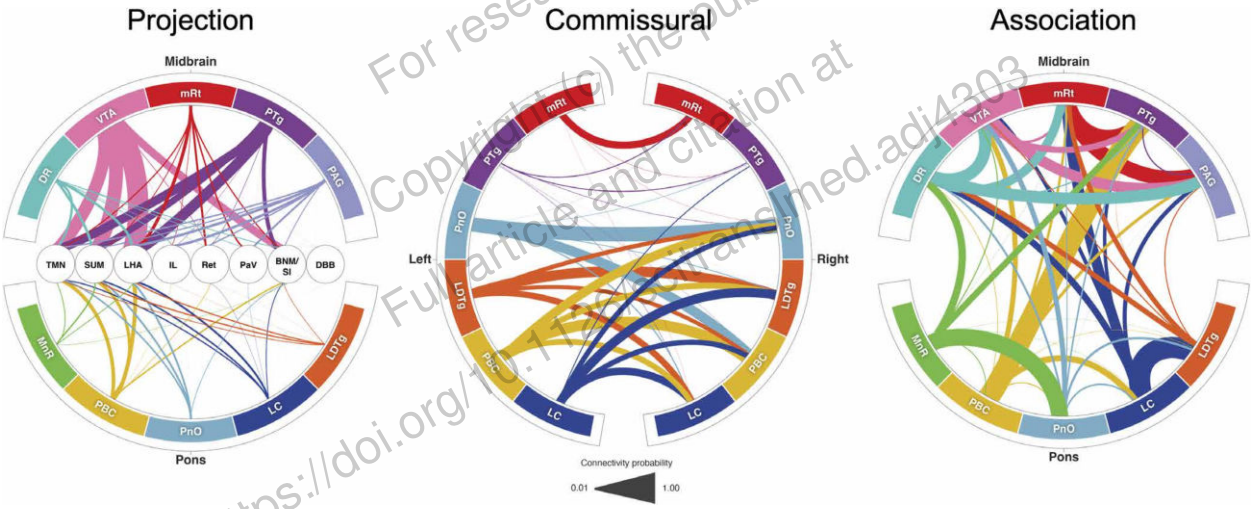

Authors' accepted version
For research purposes only
Copyright (c) the publisher
Full article and citation at
https://doi.org/10.1126/sciadv.adj4303

Fig. 4. dAAN connectograms. Projection pathways (left) connect brainstem nodes to hypothalamic, thalamic, and basal forebrain nodes. Commissural pathways (middle) connect contralateral brainstem nodes. Association pathways (right) connect ipsilateral or midline brainstem nodes. Brainstem dAAN nodes are shown in the outer ring of all connectograms. In the projection connectogram, the hypothalamic, thalamic, and basal forebrain nodes are shown in the center: TMN, SUM, LHA, IL, Ret, PaV, BNM/ SI, DBB. Line thicknesses in each connectogram are proportional to the CP value derived from probabilistic tractography analysis. For clarity of visualization, interspecimen mean in CP measurements is shown in the connectograms. In the commissural connectogram, we show the connections from left to right and omit the right-to- left connections for ease of visualization. In the association connectogram, we take a mean of left-and right-sided connectivity for bilaterally represented nodes. We do not show a connectogram for projection pathways to the DMN nodes because the CP values are lower than for diencephalic and forebrain projection pathways (table S11), such that connections would not be visualizable at this scale.

sevennetwork Yeo atlas (Table S12). Mean connectivity between the entire dAAN and DMN was greater than connectivity between the dAAN and the visual and limbic networks but less than connectivity between the dAAN and the dorsal attention, ventral attention (i.e., salience), executive control, and somatomotor networks.

Association and commissural pathways of the dAAN

Deterministic and probabilistic tractography analyses revealed connections linking all candidate brainstem nodes with at least one ipsilateral or midline brainstem node (Fig. 4). As with the projection fiber pathways, the association fiber pathways were similar between specimens. Extensive connectivity between midline, left-sided, and right-sided brainstem candidate dAAN nodes (both reticular and extrareticular) was observed (Fig. 5 and movie S2). Quantitative connectivity data from the probabilistic tractography analyses of association pathways are provided in Tables S13 to S15.

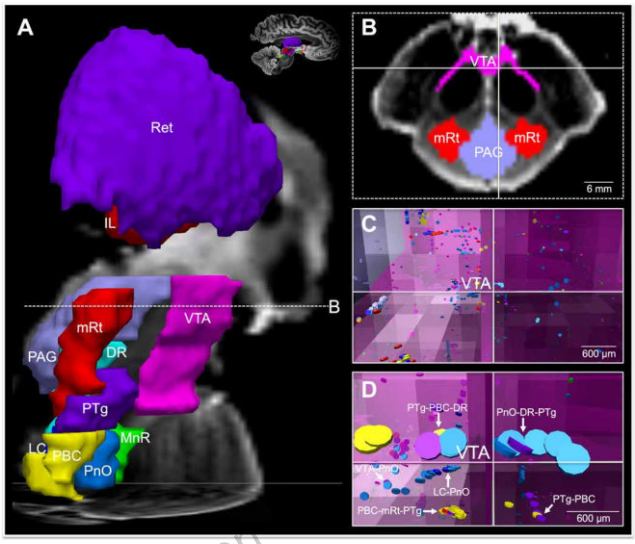

Fig. 5. Connections linking association pathways of the dAAN. Ex vivo diffusion MRI tractography data are shown for brain specimen 1. Candidate brainstem dAAN nodes are shown from a right lateral perspective in (A), superimposed upon a sagittal non–diffusion-weighted (b = 0) image at the mid-thalamus and an axial b = 0 image at the mid-pons. The dashed line in (A) represents the intercollicular midbrain level at which dAAN nodes are shown in the axial image in (B). A magnified view of the VTA is shown in (C) and is further magnified in (D), at the anatomic location indicated by the solid crossing lines in (B). The circular discs in (C) and (D) are tract end points, which represent the start points and termination points of each tract (i.e., there are two end points per tract). All tract end points are color-coded by the node from which they originate, and the VTA is rendered semitransparent so that end points can be seen within it. Tract end points from multiple candidate brainstem dAAN nodes are seen overlapping within the VTA and along its border (arrows) including the pedunculotegmental, parabrachial complex, and dorsal raphe (PTg-PBC- DR); pontis oralis, DR, and PTg (PnO-DR -PTg); VTA-PnO; PBC-mRt- PTg; locus coeruleus and PnO (LC - PnO); and PTg-PBC. Tract end point overlap does not prove synaptic connectivity but implies that two tracts terminate in close proximity, suggesting extensive dAAN connectivity within the VTA via association pathways. Additional visualization of dAAN connectivity within the VTA is provided in movie S2.

We observed fewer connections in the commissural analyses as compared with the projection or association analyses. Whereas projection and association tracts were distributed in multiple discreet pathways (e.g., DTT_M, DTT_L, VTT_R, and VTT_C), the commissural tracts were mostly seen within a single pathway traveling across the posterior commissure in the midbrain (Fig. S13). Additional commissural tracts outside the posterior commissure, particularly those in the pons, did not coalesce into discrete bundles of tracts. Quantitative connectivity data from the probabilistic tractography analyses of commissural pathways are provided in Table S16.

Functional connectivity between the dAAN and DMN

We used 7-T resting-state fMRI data from 84 healthy control subjects scanned in the Human Connectome Project (*45*) to investigate the functional connectivity of the DMN with subcortical

Author's accepted version
For research purposes only
Copyright (c) the publisher
Full article and citation at
https://doi.org/10.1126/sciadv.aay6485

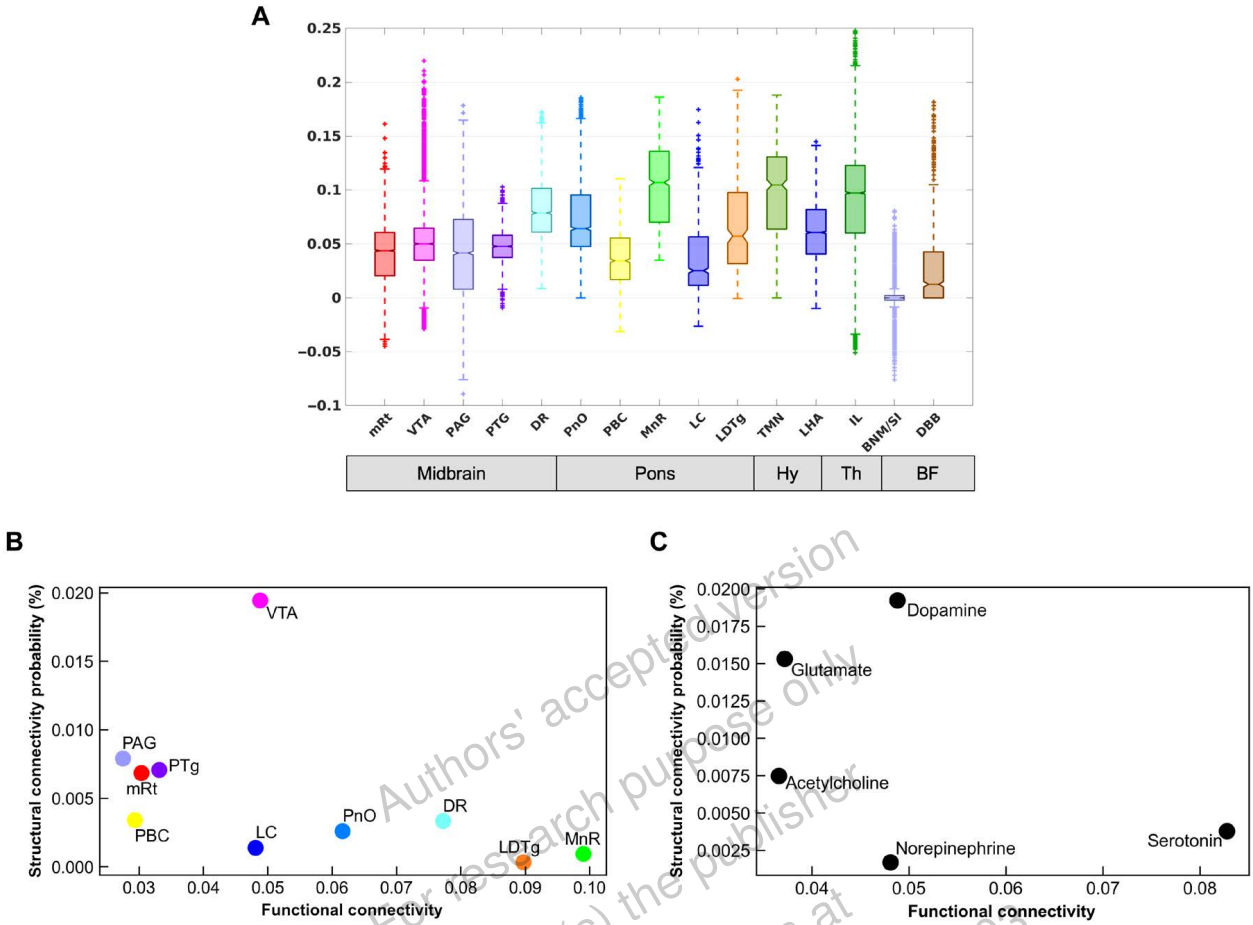

Fig. 6. Functional connectivity between subcortical dAAN nodes and cortical DMN nodes and their relationship to structural connectivity. (A) Boxplots of DMN functional connectivity for each dAAN node. Y axis represents the strength of functional connectivity (unitless) relative to the strength of cortical connectivity within the DMN. VTA voxels showed the highest level of maximal functional connectivity with the DMN, whereas MnR had the highest level of median connectivity with the DMN. (B) Scatter plot between the mean of functional connectivity (x axis) and the structural CP (y axis) for each brainstem nucleus. (C) Similar scatter plot, with brainstem nuclei grouped by the predominant type of neurotransmitter for each node, acknowledging that dAAN nodes contain neurons with diverse neurotransmitter profiles: cholinergic, PTg and LDTg; dopaminergic, VTA; glutamatergic, PBC, mRt, and PnO; noradrenergic, LC ; serotonergic, MnR and DR.

Authors' accepted version
For research purpose only
Full article and citation at
https://doi.org/10.1162/netn_a_00205
Content (c) the publisher

dAAN nodes. To map the DMN functional connectivity profile for each dAAN node, we used version 2.0 of the Harvard ascending arousal network atlas (*11*) for brainstem nuclei. We used a previously published probabilistic segmentation atlas (*46*) for thalamic nodes and an atlas proposed by Neudorfer *et al.* (*47*) for basal forebrain and hypothalamus nodes.

For each candidate brainstem, hypothalamic, thalamic, and basal forebrain node of the dAAN, we plotted the distributions of the DMN connectivity (Fig. 6A). These analyses revealed a broad range of DMN connectivity within each candidate dAAN node. Several dAAN nodes contained voxels with positive correlations and negative correlations (i.e., anticorrelations) with the DMN. Within the brainstem, the VTA demonstrated the highest level of maximal DMN connectivity, whereas MnR showed the highest median level of DMN connectivity. Within the hypothalamus, thalamus, and basal forebrain, the IL nuclei in the central thalamus demonstrated the highest level of maximal

DMN connectivity, whereas the TMN nucleus in the hypothalamus showed the highest median level of DMN connectivity.

Given the complex relationship between structural and functional connectivity in cortical networks (*48*, *49*) and the lack of data regarding structural-functional connectivity associations in subcortical networks, we plotted the relationship between functional connectivity mapped with in vivo 7-T resting-state fMRI and structural connectivity mapped with ex vivo diffusion MRI (Fig. 6, B and C) for connections between brainstem dAAN nodes and the cortical DMN. In these analyses, the DMN was analyzed as a single target region of interest. These structural-functional correlation plots revealed that several dAAN nodes, such as LDTg, MnR, and DR, had a high ratio of functional to structural connectivity, whereas other dAAN nodes, such as PAG, mRt, PTg, and PBC, had a high ratio of structural to functional connectivity. When grouping dAAN nodes on the basis of their predominant neurotransmitter (acknowledging that dAAN nodes contain neurons with variable neurotransmitter expression profiles), serotonin and norepinephrine had high ratios of functional to structural connectivity, whereas glutamate had a high ratio of structural to functional connectivity.

Authors' accepted version
For research purpose only
Copyright (C) the publisher
Full article and citation at
https://doi.org/10.1126/scitranslmed.add4203

DISCUSSION

In this multimodal brain imaging study, we mapped the connections of a proposed subcortical network that sustains resting wakefulness in human consciousness. We provide evidence for a human dAAN composed of interconnected nodes linking brainstem, hypothalamic, thalamic, and basal forebrain nuclei that are known from prior animal and human studies to sustain resting wakefulness. Further, we identified patterns of extensive interconnectivity between subcortical dAAN nodes and cortical networks that contribute to conscious awareness, including the DMN, providing a putative architecture for the integration of arousal and awareness in human consciousness.

Consistent with prior human (*19*) and animal (*18*, *20*, *21*, *50*) studies, convergent structural connectivity data from ex vivo diffusion MRI tractography and functional connectivity data from in vivo 7-T resting-state fMRI revealed that a midbrain dAAN node, the dopaminergic VTA, is a widely connected hub node at the nexus of subcortical arousal and cortical awareness networks. The VTA displayed extensive connectivity with other subcortical dAAN nodes and with cortical DMN nodes via multiple projection, association, and commissural pathways. Historically, the VTA was believed to mainly modulate behavior and cognition (*50*), but recent evidence from pharmacologic (*51*, *52*), electrophysiologic (*18*), optogenetic (*20*, *21*), and chemogenetic (*53*) methods, as well as behavioral experiments in dopamine knock-out mice (*54*), indicates that the VTA also modulates wakefulness. Functional connectivity studies from humans with disorders of consciousness further support the idea that the VTA modulates states of arousal via interactions with cortical DMN nodes (*19*). Our ex vivo diffusion MRI findings provide a structural basis for these functional observations in animals and humans, and our in vivo resting-state fMRI findings

provide further evidence for VTA-DMN connectivity, because VTA voxels showed the highest level of maximal functional connectivity of any brainstem dAAN node.

These synergistic structural-functional connectivity findings solidify the role of dopaminergic VTA neurons in modulation of wakefulness, a core component of consciousness (*55*). Our observations also reinforce ongoing efforts to target the dopaminergic VTA in therapeutic trials for patients with disorders of consciousness. Dopamine agonists and reuptake inhibitors are among the most commonly used pharmacologic therapies for patients with disorders of consciousness (*56*), and there is growing interest in using dopaminergic neuroimaging biomarkers to select patients for targeted therapies in clinical trials (*57–59*).

Connections between brainstem arousal nuclei have been demonstrated using a variety of tract-tracing and electrophysiological techniques in multiple animal species (*41*, *60–64*), but prior evidence of such interconnectivity is limited in the human brain (*42*, *65*). Here, we provide structural and functional connectivity evidence for multiple dAAN association pathways (i.e., connections between ipsilateral brainstem nuclei) and commissural pathways (i.e., connections between contralateral brainstem nuclei). Moreover, we expand upon prior observations pertaining to projection pathways of human brainstem arousal nuclei (i.e., connections between brainstem nuclei and the thalamus, hypothalamus, basal forebrain, and cerebral cortex) (*11*, *66–68*). We identified four projection pathways that connect the human brainstem to the diencephalon and forebrain: VTT_C, VTT_R, DTT_M, and DTT_L. The anatomic trajectories and connectivity patterns of these dAAN projection pathways are consistent with prior studies of human brainstem connectivity (*11*, *42*, *69*) and are similar to their rodent (*41*, *70*), feline (*64*, *71*), and primate (*63*) homologs.

Our observation of direct connections between brainstem arousal nuclei and the cerebral cortex in the human brain is also consistent with extensive evidence in animal species (*62*, *63*, *72–77*). We found that the MFB and LFB are the primary pathways by which the human brainstem and cerebral cortex are connected, building on prior observations about the human MFB (*42*, *66*, *78*, *79*) and LFB (*42*). In the human brain, the MFB travels through the hypothalamus and basal forebrain, carrying short-range tracts that connect with hypothalamic and basal forebrain nuclei via the VTT_C. Long-range MFB fibers continue on to the cerebral cortex, connecting with DMN nodes within the frontal lobes. Although elucidation of the functional subspecialization of MFB and VTT_C pathways in the human brain awaits future investigation, these structural connectivity results are consistent with wake-promoting brainstem-hypothalamus-basal forebrain circuits in animals (*12*).

We found that the LFB is the primary pathway by which human dAAN nodes connect with temporoparietal DMN nodes, including the PMC (i.e., posterior cingulate cortex and precuneus), a hub node within the DMN whose connectivity is believed to be necessary for conscious awareness (*13*). Functional connectivity between the VTA and the PMC was recently shown to modulate consciousness in patients with severe brain injuries and healthy volunteers receiving propofol sedation (*19*), observations that are supported by our VTA-PMC connectivity findings. However, we also identified extensive DMN connectivity between multiple brainstem dAAN nodes beyond the VTA, with particularly strong connectivity in the PMC and MPFC nodes. The

Authors' accepted version
For research purposes only
Copyright (c) this publisher
Full article and citation at
https://doi.org/10.1126/sciadv.adq1803

functional significance of these differential DMN connectivity patterns is unknown and requires future studies to evaluate the relative contributions of brainstem dAAN nuclei to modulating the DMN in the resting, conscious human brain.

This study has several limitations. The small number of brain specimens ($n = 3$) underscores the need for confirmatory studies with larger sample sizes. The voxel size that we used was almost 1000 times larger in dimension than the diameter of a single axon (~600 to 750 μm versus ~1 μm). Hence, the tractography results reported here do not represent "ground-truth" axonal anatomy. All tractography results should be considered inferential and are subject to the inherent methodological limitations of diffusion MRI tractography, which have been well characterized (*80–84*). Another limitation is that diffusion tractography cannot determine the direction of electrical signaling within a tract. There is extensive electrophysiological evidence for "top-down" modulation of arousal (*85*, *86*) and cognition (*87*), and the MFB is known to carry descending fibers alongside its ascending fibers (*88*). In addition, multiple types of neurons within the arousal network may have bifurcating axons with ascending and descending projections (*76*). Thus, our use of the term "ascending" is not intended to suggest that arousal is mediated solely by ascending pathways from the brainstem to rostral sites. Notably, falsepositive tracts can be generated by a "highway effect" whereby tracts that run alongside one another can merge into anatomically implausible pathways. Conversely, false-negative findings can occur because of a variety of factors, including increased distance between nodes and tractography's low sensitivity for identifying axons with multidirectional branching patterns (*89*, *90*), small diameters (*63*), or lack of myelination (*63*). These latter anatomic features are known characteristics of the rostral serotonergic, noradrenergic, and cholinergic axonal projections, which may explain the absent or uncertain connectivity findings for MnR, LC, and LDTg (Table 1).

We also acknowledge that the present study does not address functional subspecialization, or fractionation, of different circuits within the dAAN. Given that dAAN nodes contain neurons using multiple neurotransmitters (*8*), there is substantial intranodal functional complexity that is not accounted for in our structural connectivity methods, which treat each node as a singular entity. Fractionation of dAAN circuits will require future functional brain mapping studies, just as fractionation of DMN circuits was performed in the years after the DMN's discovery (*91*, *92*). Given the limitations of the present work, we believe that the anatomic resources provided here will be most useful if integrated with complementary neuroimaging and immunohistochemical atlases of the human brainstem (*93–96*). Together, these resources provide a foundation for filling the resolution gap between the mesoscale connectome and microscale synaptome.

In conclusion, we provide insights into the connectivity of a subcortical arousal network that sustains resting wakefulness in the conscious human brain. We found that subcortical dAAN nodes interconnect with cortical DMN nodes, as well as the nodes of widely distributed networks throughout the cerebral cortex, providing a neuroanatomic basis for integration of arousal and awareness in human consciousness. We propose that the network-based autopsy methods and connectivity data generated here could advance the study of coma pathogenesis and recovery (*1*).

Authors' accepted version
For research purposes only
Copyright (c) the publisher
Full article and citation at
https://doi.org/10.1126/sciadv.adj4503

Classification of projection, association, and commissural pathways within the human dAAN will allow categorization of different combinations of preserved pathways in patients who recover from coma. This effort may ultimately enable identification of the minimum ensemble of nodes and connections that are sufficient for sustaining wakefulness in human consciousness.

MATERIALS AND METHODS

Study design

In this study, we performed ex vivo MRI scans of three human brain specimens to map the connectivity of a proposed arousal neural network, the dAAN. We then compared structural connectivity maps derived from these three ex vivo diffusion MRI datasets to functional connectivity maps derived from a 7-T resting-state fMRI dataset acquired in the Human Connectome Project (*45*). Our goal with mapping this structural-functional connectivity was to identify the neuroanatomic basis for the integration of arousal and awareness in the conscious human brain.

Written informed consent for brain donation was obtained postmortem from family surrogate decision-makers, in accordance with a research protocol approved by the Institutional Review Board at Mass General Brigham (protocol no. 2010P000243). All specimens were fixed in 10% formaldehyde. Immediately before scanning, the specimens were transferred from 10% formaldehyde to Fomblin (perfluoropolyether, Ausimont USA Inc., Thorofare, NJ), which reduces magnetic susceptibility artifacts (*97*). Criteria for inclusion of brain specimens in this study were (i) no history of neurological illness, (ii) no abnormal in vivo brain scan, (iii) normal neurological examination documented by a clinician in the medical record before death, and (iv) normal postmortem gross examination of the brain by a neuropathologist. No statistical methods were used to predetermine the sample size. Identification of candidate dAAN nodes in the ex vivo MRI datasets was guided by immunohistochemistry and histology, which we performed on sections from the scanned brain specimens.

Authors' accepted version
For Research purposes only
Copyright (c) the publisher
Full article and citation at
https://doi.org/10.1126/sciadv.adj4503

Identification of candidate dAAN nodes

We identified candidate dAAN nodes via four lines of previously published evidence: electrophysiological, gene expression, lesion, and stimulation. Specifically, we identified subcortical nuclei for which prior studies demonstrated any one of the following: (i) tonic activity during resting wakefulness (*30*, *98*), (ii) increased Fos staining after periods of arousal (*99*), (iii) lesion-induced loss of resting wakefulness (*100*), or (iv) stimulation-induced arousal (Table S1) (*15*). Animal electrophysiology, gene expression, lesion, and stimulation studies were identified using reference lists from textbooks (*30*, *101–105*), review articles (*12*, *106–110*), and from the authors' reference libraries.

Ex vivo MRI data acquisition

For brain specimen 1, we dissected the hemispheres from the diencephalon and basal forebrain and dissected the cerebellum from the brainstem to fit the specimen into the small bore of a 4.7-T

MRI scanner (Bruker BioSpec), as previously described (*11*). The dissected specimen consisted of the rostral pons, midbrain, hypothalamus, thalamus, basal forebrain, and part of the basal ganglia. Specimens 2 and 3 were scanned as whole brains on a large-bore 3-T Tim Trio MRI scanner (Siemens Medical Solutions, Erlangen, Germany), using previously described acquisition parameters (*111*). Details regarding the diffusion MRI sequences used on the 4.7and 3-T MRI scanners are provided in the Supplementary Materials.

Cortical surface generation and parcellation of DMN nodes

To generate cortical surfaces for parcellation of DMN nodes, we acquired multi-echo flash (MEF) data at 1-mm isotropic resolution on the 3-T Tim Trio MRI scanner during the same scanning session during which the diffusion data were acquired. Details regarding the MEF sequence parameters are provided in the Supplementary Materials. To generate the cortical surface model, we synthesized a proton density (PD) volume from the MEF dataset and removed background noise by thresholding the PD volume to create a mask containing hyperintense voxels. The mask was then subtracted from the initial PD volume to achieve a more homogeneous image. Using the intensity-corrected PD volume, we generated white and gray matter segmentations using the modified Sequence Adaptive Multimodal Segmentation (SAMSEG) pipeline (*112*). The SAMSEG white and gray matter segmentations were then used to generate the pial and white matter surfaces.

Once the surfaces were generated, we parcellated the cortical nodes of the DMN in whole-brain specimens 2 and 3 for the dAANDMN connectivity analysis. DMN nodes were parcellated according to the seven-network Yeo atlas (*113*), as instantiated in the 1000node Schaefer version of the atlas (*114*): PMC (i.e., posterior cingulate cortex and precuneus), MPFC, IPL, lateral temporal lobe (LT), and medial temporal lobe (MT). To translate the surface-based MEF labels into volumetric diffusion space, we used a boundary-based registration method (*115*) with a nonlinear spherical transformation model, available through FreeSurfer (*116*). We then projected the Yeo DMN atlas labels from the pial surface, in a perpendicular direction at 2-mm depth, into volumetric space.

The DMN nodes of the seven-network Yeo atlas (*113*) may include subregions with heterogeneous functions. The large size of the Yeo atlas nodes is relevant to the neuroanatomic interpretation of the data presented here because data from human electrophysiologic (*117*) and fMRI (*118*, *119*) studies, as well as nonhuman primate tract-tracing studies (*120*), suggest that the DMN may involve only the ventral component of the precuneus, as opposed to the ventral and dorsal components of the precuneus that are included in the PMC node from the seven-network Yeo atlas (Fig. S14). Similarly, the MPFC, IPL, and MT nodes of the Yeo atlas may be parcellated into DMN subnetworks (i.e., a midline core, a dorsal MPFC subsystem, and a MT subsystem) that subserve different aspects of internally directed cognition (*91*, *92*). Future studies that map dAAN connectivity with these DMN subregions have the potential to provide more granular insights into the structural and functional properties of human arousal and awareness. Last, in a post hoc analysis with the goal of comparing dAAN-DMN connectivity with dAAN connectivity to other cortical networks, we performed a similar surface-based atlas registration of the six remaining

Authors' accepted version
For research purpose only
Copyright (c) the publisher
Full article and citation at
https://doi.org/10.1126/sciadv.adh4305

cortical networks defined in the seven-network Yeo atlas: visual, somatomotor, dorsal attention, ventral attention (i.e., salience), limbic, and executive control.

Detailed processing parameters are provided in our code, which can be accessed at https://zenodo.org/records/10360878 (*121*). All data were processed using a standard release of FreeSurfer 7.1.2, available at https://github.com/freesurfer/freesurfer, and FSL 6.0.3, available at https://fsl.fmrib.ox.ac.uk/fsl/fslwiki.

Sectioning and staining for histologic-radiologic correlations

Upon completion of ex vivo MRI data acquisition, brain specimen 1 was divided into seven blocks, which were embedded in paraffin. We then cut serial transverse sections of the rostral pons and midbrain and coronal sections of the hypothalamus, thalamus, and basal forebrain at 10-μm thickness (LEICA RM2255 microtome, Leica Microsystems, Buffalo Grove, IL, USA). Every 50th section was stained with hematoxylin and eosin for nuclei and counterstained with Luxol fast blue for myelin, yielding a stained section every 500 μm. The purpose of these stains was to define the neuroanatomic location, borders, and morphology of all candidate dAAN nodes. In addition, 10-μm sections from the midbrain were prepared using tyrosine hydroxylase (Pel-Freez Biologicals; rabbit polyclonal P40101) and counterstained with hematoxylin, and 10-μm sections from the pons were prepared using tryptophan hydroxylase (Sigma-Aldrich; mouse monoclonal AMAB91108) and counterstained with hematoxylin. Tyrosine hydroxylase more precisely characterizes the location, borders, and morphology of the dopaminergic VTA, as detailed in the Supplementary Materials. Tryptophan hydroxylase characterized the location, borders, and morphology of the serotonergic MnR and DR.

Authors' accepted version
For research purpose only
Copyright (c) the publisher
Full article and citation at
https://doi.org/10.1126/scitranslmed.adi4303

Histology-guided neuroanatomic localization of brainstem dAAN nodes

For brain specimen 1, candidate dAAN nodes (i.e., nodes selected on the basis of the a priori criteria) were traced on the diffusionweighted images using histological guidance. Each diffusion image was compared to its corresponding histological section to ensure that radiologic dAAN nodes shared the same location and morphology as the histological dAAN nuclei (Figs. S4 and S5). Histological nuclei were delineated by visual inspection of their cytoarchitecture with a light microscope and with digitized slides. We then crossreferenced with the Paxinos atlas of human brainstem neuroanatomy for brainstem dAAN nodes (*39*) and with the Allen Institute atlas of the human brain for thalamic, hypothalamic, and basal forebrain dAAN nodes (*40*). Because brainstem nuclei change shape, size, and contour along the rostro-caudal axis, histological guidance of dAAN node tracing was performed for every axial diffusion image using its corresponding histological section, yielding a 3D model of brainstem arousal nuclei.

For brain specimens 2 and 3, the brainstem dAAN nuclei were also traced manually on each diffusion MRI dataset but with reference to canonical atlases and selected immunostains, not serial immunostains or comprehensive histological data. Specifically, the neuroanatomic boundaries of brainstem nodes were visually confirmed with respect to two reference templates: (i) the ex vivo template of histologically guided nodes generated for specimen 1, which we release here as part

of the Harvard Disorders of Consciousness Histopathology Collection (http://histopath.nmr.mgh.harvard.edu); and (ii) the Paxinos human brainstem atlas (39).

Histology-guided neuroanatomic localization of diencephalic and forebrain dAAN nodes

Similar to the brainstem nucleus segmentation, we used histological guidance via coronal sections through the diencephalon and basal forebrain to identify the borders of thalamic, hypothalamic, and basal forebrain dAAN nodes on the diffusion MRI dataset for brain specimen 1. To segment the thalamic, hypothalamic, and basal forebrain nuclei for specimens 2 and 3, we manually traced each node based on the Allen Institute human brain atlas (*40*).

Overview of ex vivo diffusion MRI data processing for tractography

We processed the ex vivo diffusion MRI datasets for deterministic and probabilistic tractography analyses to generate insights into both qualitative anatomic relationships of dAAN tracts and quantitative dAAN connectivity properties. Deterministic tractography yields more visually informative qualitative data about the neuroanatomic relationships between tracts (e.g., sites of tract branching and crossing) (*42*, *122*), whereas probabilistic tractography provides a more reliable quantitative measure of connectivity between nodes because it accounts for uncertainty in tract trajectories and can detect tracts on and past gray matter boundaries (*123*).

Diffusion data from all three specimens were processed for deterministic fiber tracking using Diffusion Toolkit 6.3, and diffusion data from specimens 2 and 3 were processed for probabilistic fiber tracking using FMRIB's Diffusion Toolbox, version 6.0.6. Specimen 1 was excluded from the probabilistic tractography analysis because it was scanned using different acquisition parameters, which precludes comparison of quantitative probabilistic data with specimens 2 and 3 without complex modeling that falls outside of the scope of these experiments. To optimize consistency across methods, we standardized the deterministic and probabilistic processing parameters wherever possible. Details regarding the processing and analysis parameters for deterministic and probabilistic tractography are provided in the Supplementary Materials.

Proposed neuroanatomic taxonomy for the human dAAN

We classified dAAN connections as projection, association, or commissural. This classification system is intended for use as a neuroanatomic taxonomy for the subcortical dAAN, akin to that of cortical networks whose connections are classified in these terms (*43*). In the cortical classification system, the cortex is the frame of reference for defining fiber pathways. Projection fibers project from the cortex to subcortical regions. Association fibers connect ipsilateral cortical regions, and commissural fibers cross the midline to connect contralateral cortical regions.

Here, we propose that the brainstem is the frame of reference for classifying fiber pathways of the dAAN. As such, projection fibers are defined as those that project from brainstem nuclei to rostral diencephalic nuclei, basal forebrain nuclei, or cortical regions that contribute to consciousness (i.e., DMN nodes). Association fibers connect brainstem nuclei to ipsilateral brainstem nuclei, and commissural fibers cross the midline to connect with contralateral brainstem nuclei.

Authors' accepted version
For research purposes only
Copyright (c) the publisher
Full article and citation at
https://doi.org/10.1126/sciadv.abj3503

7-T resting-state fMRI of dAAN-DMN connectivity

Seven-tesla resting-state fMRI scans from 84 healthy controls in the Human Connectome Project (*45*) were used in this study. The resting-state fMRI data were minimally preprocessed, resampled, and co-registered to the MNI template by the Human Connectome Project pipeline (*124*). Grayordinate representations of the data were used for joint analysis of cortical and subcortical connectivity, where cortical data were sampled onto the subject surface, and subcortical data were represented in volumetric space (*124*). We did not apply any further spatial smoothing to the minimally preprocessed data because typical Gaussian smoothing would mix signals across different functional regions (*125*), which may make it difficult to resolve functional relationships between dAAN nodes (*126*). Instead, an improved signal-to-noise ratio was obtained using a tensor-based group analysis, as described below.

Using our previously developed pipeline (*127*), we estimated functional connectivity from the dAAN to the canonical DMN. Specifically, we first temporally synchronized the resting-state fMRI data of each control to a group average using the group BrainSync algorithm (*128*, *129*). We further arranged the synchronized data from all subjects along the third dimension (the first dimension is space, and the second dimension is time), forming a 3D data tensor. We then applied the Nadam-Accelerated SCAlable and Robust (NASCAR) tensor decomposition method (*130*, *131*) to identify the whole-brain DMN. The subcortical section was separated from the grayordinate structure and converted to a volumetric NIFTI file.

To extract the connectivity profile for each nucleus in the dAAN, we used version 2.0 of the Harvard ascending arousal network atlas (*11*) for brainstem nuclei, the probabilistic segmentation atlas (*46*) for thalamic nuclei, and an atlas proposed by Neudorfer *et al.* (*47*) for basal forebrain and hypothalamic nuclei to define the regions of interest. We then, for each region of interest, plotted the distributions of the DMN connectivity values using box plots. Of note, three candidate diencephalic dAAN nodes—SUM, PaV, and Ret—were not included in the MRI atlases.

Author's accepted version
For research purposes only
Copyright (C) the publisher
Full article and citation at
https://doi.org/10.1126/scitranslmed.adj2053

Statistics

Using the probabilistic tractography data from the ex vivo diffusion MRI scans in specimens 2 and 3, we computed an undirected CP for each pair of nodes (i.e., node A and node B), whereby $CP_{A \leftrightarrow B}$ represents the probability of a tract connecting node A and node B, weighted by the number of voxels within each node and invariant to direction (*69*). Although complete elimination of false-positive tracts (i.e., anatomically implausible connections) is not possible with probabilistic tractography, we attempted to account for the possibility of false-positive tracts by comparing CP values for each candidate brainstem dAAN node with two control nodes: the basis pontis (BP) and the red nucleus (RN). On the basis of prior anatomic labeling studies in animal models, the BP and RN are not expected to have substantial connectivity with the candidate brainstem dAAN nodes (*41*), because they mainly contain corticospinal and corticopontocerebellar fibers that connect the cerebellum to the primary motor cortex (and vice versa), the primary function of which is motor activity (*132*). We established two a priori criteria, both of which must be met, for operationally defining a structural connection between a pair of candidate dAAN nodes (nodes A and B): (i)

$CP_{A\leftrightarrow B} > 0$; and (ii) the 95% CI for $CP_{A\leftrightarrow B}$ must not overlap with the 95% CI for any of the following: $CP_{A\leftrightarrow BP}$, $CP_{A\leftrightarrow RN}$, $CP_{B\leftrightarrow BP}$, and $CP_{B\leftrightarrow RN}$. Details regarding calculation of the 95% CI for each CP measurement, which were calculated by modeling CP as a binomial distribution, are provided in the Supplementary Materials. Because of the conservative nature of this analysis, we did not perform multiple-hypothesis correction.

REFERENCES AND OTHER INFORMATION

https://www.science.org/doi/abs/10.1126/scitra nslmed.adj4303

Authors' accepted version
For research purpose only
Copyright (c) the publisher
Full article and citation at
https://doi.org/10.1126/scitranslmed.adj4303